

ON THE SCATTERING OF ELECTROMAGNETIC WAVES BY A CHARGED SPHERE

J. Klačka

Faculty of Mathematics, Physics and Informatics
Comenius University
Mlynská dolina, Bratislava 84248, Slovak Republic

M. Kocifaj

ICA, Slovak Academy of Sciences
Dúbravská cesta, Bratislava 84503, Slovak Republic

Abstract—Scattering of electromagnetic radiation by a charged homogeneous spherical particle/body is treated. Theoretical solution represents a generalization of the Mie's scattering theory for electrically neutral sphere. It is shown that classical and quantum physics approaches may lead to different conclusions, as documented by numerical computations assuming various permeabilities, refractive indices, surface charges, temperatures, and other physical parameters of the spherical particles. Two discrete wavelengths ($5\ \mu\text{m}$ and $1\ \text{mm}$) of the incident radiation are considered. Optical properties of charged particles composed of absorbing and slightly absorbing materials can essentially differ. Especially, the resonance peaks typically occur when imaginary part of particle refractive index is low. The relative permeability of a material may differ from unity at large wavelengths, e.g., in microwave region. Basically, the relative permeability appears to be less important factor than the surface charge. However, the permeability can influence the scattering and extinction efficiencies, as well as the backscattering features of small particles, under some conditions.

1. INTRODUCTION

The scattering of electromagnetic waves by a spherical electrically neutral particle/body was elaborated by Mie [1]. Much later Bohren and Hunt [2] addressed the effect of surface charge on the optical features of small homogeneous spherules. Just recently Klačka and Kocifaj [3] partially improved the physics of this phenomena and demonstrated the optical consequences on set of examples assuming charged and electrically neutral (Mie) particles. Now, some extension to the theory is suggested. Specifically, it deals with the motion of free electrons on the surface of a spherical particle [4, 5]. We incorporate the new suggestions into a general theory and present results of numerical calculations for scattering on spherical particle with various values of permeability. The classical and quantum physics approaches are applied to the electromagnetic scattering problem showing the important differences.

2. FUNDAMENTAL EQUATIONS FOR THE MODEL

Fundamental equations are represented by Maxwell equations, material relations and boundary conditions.

2.1. Material Relations in Uniform Isotropic Media

In the following the subscript 1 refers to a spherical particle, and, the subscript 2 is reserved for the medium surrounding the particle.

For both media (the particle and its surrounding) we can write:

$$\begin{aligned}\vec{D}_k &= \varepsilon_k \vec{E}_k, \\ \vec{B}_k &= \mu_k \vec{H}_k, \\ \vec{j}_k &= \sigma_k \vec{E}_k, \quad k = 1, 2,\end{aligned}\tag{1}$$

where $\varepsilon_1, \varepsilon_2$ are electric permittivities, and μ_1, μ_2 are magnetic permeabilities. The third pair of the relations corresponds to differential form of the Ohm's law (σ_1 and σ_2 are conductivities of the materials). Moreover,

$$\vec{K} = \sigma_s \vec{E}_{\text{tangential}},\tag{2}$$

where \vec{K} is the surface current density and σ_s is the surface conductivity.

2.2. Maxwell Equations

Maxwell equations form a fundamental basis to solution of the electromagnetic scattering by a homogeneous isotropic medium. Using Eq. (1), we immediately obtain the relevant set of equations:

$$\begin{aligned}
 \nabla \cdot \vec{E}_k &= \rho_k / \varepsilon_k, \\
 \nabla \cdot \vec{H}_k &= 0, \\
 \nabla \times \vec{E}_k + \mu_k \frac{\partial \vec{H}_k}{\partial t} &= 0, \\
 \nabla \times \vec{H}_k &= \sigma_k \vec{E}_k + \varepsilon_k \frac{\partial \vec{E}_k}{\partial t}, \\
 \frac{\partial \rho_k}{\partial t} + \sigma_k \nabla \cdot \vec{E}_k &= 0, \quad k = 1, 2,
 \end{aligned} \tag{3}$$

where the last one is the continuity equation. The first of Eq. (3) and the continuity equation guarantee that no free volume charge exists in the media, i.e., $\rho_k = 0$.

2.3. Fundamental Boundary Conditions for the Model

Let us consider a sphere in a vacuum, $\varepsilon_2 = \varepsilon_0$, $\mu_2 = \mu_0$, $\sigma_2 = 0$. According to Mishchenko et al. [6] $\vec{K} = 0$ for media with finite conductivity. However, if the skin depth $D = \sqrt{2/(\omega\mu_1\sigma_1)}$ [16] is much smaller than the particle radius (ω is an angular frequency), the surface current \vec{K} has to be taken into account in the boundary conditions. On the basis of Eqs.(1)–(3), we can write:

$$\begin{aligned}
 (\varepsilon_0 \vec{E}_2 - \varepsilon_1^* \vec{E}_1) \cdot \vec{n} &= \eta_0 - \frac{i}{\omega} \nabla_s \cdot \vec{K}, \\
 (\mu_0 \vec{H}_2 - \mu_1 \vec{H}_1) \cdot \vec{n} &= 0, \\
 \vec{n} \times (\vec{E}_2 - \vec{E}_1) &= 0, \\
 \vec{n} \times (\vec{H}_2 - \vec{H}_1) &= \vec{K},
 \end{aligned} \tag{4}$$

where $\varepsilon_1^* = \varepsilon_1 + i\sigma_1/\omega$, $\eta_0 = Q/(4\pi R^2)$ for the spherical particle of radius R and the net surface charge Q , and, $\nabla_s \cdot \vec{K} = \{\partial K_\varphi / \partial \varphi + \partial(K_\vartheta \sin \vartheta) / \partial \vartheta\} / (R \sin \vartheta)$ in spherical polar coordinates, (ϑ and φ are polar and azimuthal angles) (consult also Eqs. (15), (16) in [17]). Further, $\eta = \text{Re}\{\tilde{\eta} \exp(-i\omega t)\}$, where η is surface charge density, $\eta \equiv \eta(\vec{r}, t)$, and $\int \tilde{\eta} dA = 0$, $\tilde{\eta} \equiv \tilde{\eta}(\vec{r})$. The time dependency of the incident radiation fields (electric and magnetic) is $\exp(-i\omega t)$. The

transition from general form of boundary conditions (Eq. (4)) to the conventional Mie's formulation is given by $\eta_0 = 0$, $\eta \equiv 0$, $\vec{K} \equiv 0$.

3. SCATTERING COEFFICIENTS

To characterize the optical behavior of a scattering particle, the far-field zone formalism is traditionally considered [7]. In the far-field region the electric field vector is perpendicular to the direction of propagation, and, transversal components of the electric and magnetic fields approach zero as $1/r$, where r is the distance from the particle. At the particle surface the tangential components of the total electric field are continuous (\vec{E}_2 is the sum of the incident and scattered fields and \vec{E}_1 is the internal field). Application of boundary conditions represented by Eq. (4) to the electric and magnetic fields finally yields for the scattering coefficients a_n and b_n (see [3]):

$$a_n = \frac{\psi'_n(mx) \left[\frac{\psi_n(x)}{\mu_0} - \frac{i\omega\sigma_s\psi'_n(x)}{k} \right] - \psi_n(mx) \frac{m\psi'_n(x)}{\mu_1}}{\psi'_n(mx) \left[\frac{\xi_n(x)}{\mu_0} - \frac{i\omega\sigma_s\xi'_n(x)}{k} \right] - \psi_n(mx) \frac{m\xi'_n(x)}{\mu_1}},$$

$$b_n = \frac{\psi_n(mx) \left[\frac{\psi'_n(x)}{\mu_0} + \frac{i\omega\sigma_s\psi_n(x)}{k} \right] - \psi'_n(mx) \frac{m\psi_n(x)}{\mu_1}}{\psi_n(mx) \left[\frac{\xi'_n(x)}{\mu_0} + \frac{i\omega\sigma_s\xi_n(x)}{k} \right] - \psi'_n(mx) \frac{m\xi_n(x)}{\mu_1}}, \quad (5)$$

$$\psi_n(\varrho) = \varrho j_n(\varrho), \quad \xi_n(\varrho) = \varrho h_n^{(1)}(\varrho),$$

where $x = kR$, $mx = KR$, $K = \omega\sqrt{\mu_1\varepsilon_1^*}$ and the prime denotes differentiation with respect to the argument of the special function. The $j_n(\varrho)$ and $h_n^{(1)}(\varrho)$ are spherical Bessel and Hankel functions of the first kind, respectively [18]. In Eq. (5) $k = \omega/c$ is the wavenumber, c is the speed of light in vacuum, and $\varepsilon_1^* = \varepsilon_1 + i\sigma_1/\omega$.

The amount of radiative energy that is removed or scattered by the particle is traditionally related to its projection area, which is πR^2 for ideal sphere. Following the above concept, the cross sections for extinction and scattering, C_{ext} and C_{sca} , respectively, can be determined as series expansions in the scattering coefficients:

$$C_{ext} = \frac{2\pi}{k^2} \sum_{n=1}^{\infty} (2n+1) \operatorname{Re} \{a_n + b_n\},$$

$$C_{sca} = \frac{2\pi}{k^2} \sum_{n=1}^{\infty} (2n+1) \operatorname{Re} \{|a_n|^2 + |b_n|^2\}. \quad (6)$$

These formulae hold for the case $\eta_0 = 0$. The general case $\eta_0 \neq 0$, $\eta \neq 0$ can be obtained by a superposition of the stationary

fields generated by the stationary charge η_0 and by the changing charge η .

Another important quantity characterizing the force that electromagnetic radiation exerts on a spherical particle is the radiation pressure [8]. The dimensionless efficiency factor for radiation pressure is

$$Q_{pr} = Q_{ext} - Q_{sca} \langle \cos \theta \rangle, \quad (7)$$

where

$$Q_{ext} \equiv \frac{C_{ext}}{\pi R^2} = \frac{2}{x^2} \sum_{n=1}^{\infty} (2n+1) \operatorname{Re}(a_n + b_n),$$

$$Q_{sca} \langle \cos \theta \rangle = \frac{4}{x^2} \sum_{n=1}^{\infty} \left\{ \frac{n(n+2)}{n+1} \operatorname{Re}(a_n a_{n+1}^* + b_n b_{n+1}^*) \right. \quad (8)$$

$$\left. + \frac{2n+1}{n(n+1)} \operatorname{Re}(a_n b_n^*) \right\}$$

and coefficients a_n and b_n can be determined numerically, applying the following concept

$$a_n = \frac{A_{1n} \psi_n(x) - A_{2n} \psi_{n-1}(x)}{A_{1n} \xi_n(x) - A_{2n} \xi_{n-1}(x)},$$

$$A_{1n} \equiv \left(1 + \frac{ng}{x} \right) D_n(mx) + \frac{mn}{x} \frac{\mu_0}{\mu_1},$$

$$A_{2n} \equiv m \frac{\mu_0}{\mu_1} + g D_n(mx),$$

$$b_n = \frac{B_{1n} \psi_n(x) - \psi_{n-1}(x)}{B_{1n} \xi_n(x) - \xi_{n-1}(x)}, \quad (9)$$

$$B_{1n} \equiv m \frac{\mu_0}{\mu_1} D_n(mx) + \frac{n}{x} - g,$$

$$D_n(mx) \equiv \frac{\psi'_n(mx)}{\psi_n(mx)} = \frac{\psi_{n-1}(mx)}{\psi_n(mx)} - \frac{n}{mx},$$

$$g \equiv i\omega k^{-1} \mu_0 \sigma_s.$$

Eq. (9) represents a generalization of Eq. (26) given by Klačka and Kocifaj [3]. Eq. (9) reduces to Eq. (26) given in [3] for the special case $\mu_1 = \mu_0$ (used also by Rosenkrantz and Arnon [9]). The conventional formulae for the Mie theory for electrically neutral particles follows from Eq. (9) by setting $g = 0$, i.e., when $A_{1n} = D_n(mx) + (mn/x)\mu_0/\mu_1$, $A_{2n} = m\mu_0/\mu_1$, $B_{1n} = m(\mu_0/\mu_1)D_n(mx) + n/x$. These relations can be even more simplified if one assumes that the particle is nonmagnetic, i. e., $\mu_1 = \mu_0$.

4. CONDUCTIVITY AND MOTION OF FREE SURFACE CHARGES

We will use the conventional approach determining the motion of electrons. The idea goes back to Paul Drude, and it is known as a classical phenomenological model for the conductivity, for the 3-dimensional case (see, e.g., [10], p. 93 and 95; [11], p. 88).

4.1. 3-D Case: Volume Charges

A free electrically charged particle of a mass m and electric charge q is decelerated by some sort of friction force

$$m \left(\frac{d\vec{v}}{dt} + \frac{\vec{v}}{\tau} \right) = \text{Re} \left(q\vec{E}_0 e^{-i\omega t} \right), \quad (10)$$

where τ is a coefficient describing the damping (attenuation rate is τ^{-1}). The relaxation time τ takes into account all internal losses in a lumped parameter. Eq. (10) and the equilibrium ansatz $\vec{v} = \vec{v}_0 e^{-i\omega t}$ yield

$$\vec{v}_0 = \frac{q\vec{E}_0\tau}{m} \frac{1}{1 - i\omega\tau}. \quad (11)$$

The frequency dependent conductivity σ of a metal can be determined using Ohm's law in its differential form, $\vec{j} = \sigma \vec{E} = Nq\vec{v}$, where \vec{j} is the current density and N is the concentration/density of moving charges (see also Eq. (44) in [19]). Based on Eq. (11), we have

$$\begin{aligned} \sigma(\omega) &= \frac{Nq^2}{m} \frac{\tau}{1 - i\omega\tau} = \varepsilon_0\omega_p \frac{\omega_p\tau}{1 - i\omega\tau}, \\ \omega_p^2 &\equiv \frac{Nq^2}{m\varepsilon_0}, \end{aligned} \quad (12)$$

where ω_p is the plasma frequency.

Inserting Eq. (12) into formula for ε_1^* (introduced below Eq. (4)) we obtain expression formally consistent with Eq. (8) in [15].

4.2. 2-D Case: Surface Charges

Let us assume that the surface charges are free to move anywhere on the surface, i.e., the charges are not localized around a particular point. In this case we can also use Eq. (10), but \vec{E}_0 has to be substituted by the tangential electric field $\vec{E}_{\text{tangential}}$:

$$m \left(\frac{d\vec{v}_s}{dt} + \frac{\vec{v}_s}{\tau_s} \right) = \text{Re} \left(q\vec{E}_{\text{tangential}} e^{-i\omega t} \right). \quad (13)$$

Using an analogy with the equilibrium result represented by Eq. (12), we can write surface conductivity as a solution of Eq. (13):

$$\sigma_s(\omega) = \frac{N_s q^2}{m} \frac{1}{\gamma_s - i\omega} = \frac{N_s q^2}{m} \frac{\gamma_s + i\omega}{\gamma_s^2 + \omega^2}, \quad (14)$$

$$\gamma_s \equiv \tau_s^{-1}.$$

The Ohm's law for the surface current was applied, $\vec{j}_s = \sigma_s \vec{E}_{\text{tangential}} = N_s q \vec{v}_s$, where \vec{j}_s is the surface current density and N_s is the mean number of charged particles per unit area (surface concentration).

Another form of the surface conductivity can be also obtained, following the analogy between 3-D and 2-D cases. Incorporation of Pillai's approach ([4], p. 696: Eq. (12.8)) results in

$$\sigma_s(\omega) = \frac{N_s q^2}{m} \frac{\gamma_s}{\omega} \frac{\omega - i\gamma_s}{\gamma_s^2 + \omega^2}. \quad (15)$$

Finally, the analogy between 3-D and 2-D cases based on quantum approach ([10], p. 106) leads to the result

$$\sigma_s(\omega) = \frac{N_s q^2}{m} \frac{\gamma_s - i\omega}{\gamma_s^2 + \omega^2}. \quad (16)$$

4.3. Physical Discussion

We have obtained three different results, specifically Eqs. (14)–(16). All of them fulfill

$$\sigma_s^*(\omega) = \sigma_s(-\omega), \quad (17)$$

where the star denotes complex conjugation.

4.3.1. Classical Physics

Equation (15) can be derived in a way similar to that in Sec. 5.1. However, one important difference from Pillai's approach ([4], p. 696) is that $\vec{j} = nq\vec{v}$, while Pillai suggests $\vec{j} = nq\vec{r}/\tau$ (n is concentration of electrons and \vec{r} is electron displacement from equilibrium position). Physical approach should correspond to the method presented in Sec. 5.1. This is evident also from the fact that the result given by Eq. (14) fulfills the relations

$$\begin{aligned} \sigma_s(\omega) &\equiv \sigma_{s1}(\omega) + i\sigma_{s2}(\omega), \\ \sigma_{s2}(\omega) &= -\frac{1}{\pi} \int_{-\infty}^{+\infty} \frac{\sigma_{s1}(\Omega)}{\Omega - \omega} d\Omega, \\ \sigma_{s1}(\omega) &= +\frac{1}{\pi} \int_{-\infty}^{+\infty} \frac{\sigma_{s2}(\Omega)}{\Omega - \omega} d\Omega. \end{aligned} \quad (18)$$

The result given by Eq. (15) does not fulfill Eq. (18). Eq. (18) corresponds to Hilbert's transform (see, e.g., [12], p. 227–228). In physics, Eq. (18) is also known as the Kramers and Kronig relations. We remind that the integrals in Eq. (18) are in the sense of principal values (Cauchy's principal integrals, valeur principal): $\int_{-\infty}^{+\infty} u(x)/(x-t)dx = \lim_{\delta \rightarrow 0} \int_{|t-x|>\delta} u(x)/(x-t)dx$.

Since $N_s q = \eta_0 + \eta$, Eq. (14) can be rewritten to the form

$$\sigma_s(\omega) = \frac{(\eta_0 + \eta) q}{m} \frac{\gamma_s + i\omega}{\gamma_s^2 + \omega^2}. \quad (19)$$

4.3.2. Quantum Physics

In quantum approach we have $\sigma_s(\omega)$ given by Eq. (16). The relations analogous to Eq. (18) are also fulfilled, but now the correct form is

$$\begin{aligned} \sigma_s(\omega) &\equiv \sigma_{s1}(\omega) + i\sigma_{s2}(\omega), \\ \sigma_{s2}(\omega) &= +\frac{1}{\pi} \int_{-\infty}^{+\infty} \frac{\sigma_{s1}(\Omega)}{\Omega - \omega} d\Omega, \\ \sigma_{s1}(\omega) &= -\frac{1}{\pi} \int_{-\infty}^{+\infty} \frac{\sigma_{s2}(\Omega)}{\Omega - \omega} d\Omega. \end{aligned} \quad (20)$$

The quantum approach requires integration in lower part of the complex plane. Again, the integrals in Eq. (20) should be interpreted as the meaning of Cauchy's principal integrals, again.

Accepting that $N_s q = \eta_0 + \eta$, Eq. (16) can be rewritten to the form

$$\sigma_s(\omega) = \frac{(\eta_0 + \eta) q}{m} \frac{\gamma_s - i\omega}{\gamma_s^2 + \omega^2}. \quad (21)$$

5. G-PARAMETER

For the purpose of Eq. (9), we need to calculate the g -parameter:

$$g \equiv i\omega k^{-1} \mu_0 \sigma_s. \quad (22)$$

5.1. Classical Physics

Equations (19) and (22) yield

$$g = i\omega k^{-1} \mu_0 \frac{(\eta_0 + \eta) q}{m} \frac{\gamma_s + i\omega}{\gamma_s^2 + \omega^2} = -\omega k^{-1} \mu_0 \frac{(\eta_0 + \eta) e}{m_e} \frac{\omega - i\gamma_s}{\omega^2 + \gamma_s^2}. \quad (23)$$

The last expression can be formulated in terms of an electrostatic potential Φ at the surface of a uniformly charged sphere of radius

R . Since $\Phi = Q/(4\pi\epsilon_0 R)$ and the total uniformly distributed charge $Q \approx \eta_0 \times 4\pi R^2$, Eq. (23) results in

$$g \approx \frac{e\Phi}{m_e c^2} \frac{1}{x} \times \frac{-1 + i\gamma_s/\omega}{1 + (\gamma_s/\omega)^2}, \quad (24)$$

where $x \equiv kR$, and the well-known relations were used: $\omega k^{-1} = c$, $c = 1/\sqrt{\epsilon_0\mu_0}$.

5.2. Quantum Physics

Equations. (21) and (22) yield

$$g = i\omega k^{-1} \mu_0 \frac{(\eta_0 + \eta) q}{m} \frac{\gamma_s - i\omega}{\gamma_s^2 + \omega^2} = +\omega k^{-1} \mu_0 \frac{(\eta_0 + \eta) e}{m_e} \frac{\omega + i\gamma_s}{\omega^2 + \gamma_s^2}. \quad (25)$$

Equation analogous to Eq. (24) is

$$g \approx \frac{e\Phi}{m_e c^2} \frac{1}{x} \times \frac{+1 + i\gamma_s/\omega}{1 + (\gamma_s/\omega)^2}, \quad (26)$$

where $x \equiv kR$.

5.3. Discussion on g -Parameter

We have obtained two values of the g -parameter. The first one is based on the classical physics approach with the final formula Eq. (24). The second one follows quantum physics approach resulting in Eq. (26). The difference is evident: real parts of g differ in signs.

6. γ_s -PARAMETER

The relevant results are given by Eqs. (7)–(9) and Eq. (24) or Eq. (26). The only unknown quantity is γ_s .

Klačka and Kocifaj ([3], Eq. (26)) yield

$$\begin{aligned} g &= \frac{x}{2} \frac{\omega_s^2}{\omega^2 + \gamma_s^2} \left(-1 + i \frac{\gamma_s}{\omega} \right), \\ \omega_s^2 &= 2 \frac{e}{m_e} \frac{\Phi}{R^2}, \\ \gamma_s &\approx k_B T / \hbar, \end{aligned} \quad (27)$$

where ω_s is the surface plasma frequency, Φ — electrostatic potential at the surface of a uniformly charged sphere of radius R , T is temperature of the particle, $e = 1.602 \times 10^{-19}$ C, $m_e = 9.109 \times 10^{-31}$ kg, $k_B = 1.38 \times$

$10^{-23} \text{ J K}^{-1}$ is the Boltzmann's constant, and $\hbar = 1.0546 \times 10^{-34} \text{ Js}$ is Planck's constant (divided by the factor 2π).

Equation (27) contains classical result represented by Eq. (24), but fully ignore the result of quantum physics (consult Eq. (26)). However, the value of γ_s in Eq. (27) is based on quantum physics.

6.1. Classical Approach to γ_s

Recently, Heifetz et al. [5] have presented a classical derivation of γ_s . The authors have not been satisfied by the results given in Eq. (27) since the damping constant γ_s does not relate to the properties of the medium. The authors have introduced a classical-mechanics model of the temperature-dependent damping constant $\gamma_s(T)$. They have treated the electron as a classical spherical particle that has a classical electron radius (Lorentz radius) of

$$r_e = \frac{1}{4\pi\epsilon_0} \frac{e^2}{m_e c^2}. \quad (28)$$

Finally, the authors have used an idea of a linear viscous drag for a particle in water, for the case of a water droplet. According to Stoke's law

$$\frac{m}{\tau} = 6\pi r \eta, \quad (29)$$

if Eq. (10) is used. m/τ is the coefficient of resistive force, r is the Stokes radius of the particle (radius of the spherical particle) and η is the temperature-dependent fluid viscosity. Using equation analogous to Eq. (29) for the 2-D case, Eqs. (28)–(29) yield

$$\gamma_s = 6\pi r_e \eta(T) / m_e. \quad (30)$$

The classical electron radius has the numerical value $2.82 \times 10^{-15} \text{ m}$. At 20°C the viscosity of water is $\eta = 1.0003 \times 10^{-3} \text{ Pa}\cdot\text{s}$. Thus, $\gamma_s = 5.83 \times 10^{13} \text{ rad/s}$.

6.2. Improved Classical Approach to γ_s

Let us consider that the electron is not a point particle, but a small sphere. If the charge is distributed uniformly over a spherical surface of radius a_e , then the momentum \vec{p} of the electromagnetic field of the electron moving with velocity \vec{v} is

$$\vec{p} = \frac{2}{3} \frac{1}{4\pi\epsilon_0} \frac{e^2}{a_e c^2} \vec{v}, \quad (31)$$

see, e.g., [13] (p. 32–39). Eq. (31) states that the momentum of the electromagnetic field is proportional to velocity. Thus, it is the momentum of a particle with mass

$$m_{EM} = \frac{2}{3} \frac{1}{4\pi\epsilon_0} \frac{e^2}{a_e c^2}, \quad (32)$$

which Feynman calls the “electromagnetic mass” ([13], p. 35). If all the electron’s mass is electromagnetic, then $m_{EM} = m_e$. Eq. (32) enables us to determine the radius of the small spherical shell of charge representing the electron:

$$a_e = \frac{2}{3} \frac{1}{4\pi\epsilon_0} \frac{e^2}{m_e c^2} = \frac{2}{3} r_e, \quad (33)$$

if also Eq. (28) is used.

Inserting Eq. (33) into Eq. (29) one obtains

$$\gamma_s = 6\pi a_e \eta(T)/m_e = 4\pi r_e \eta(T)/m_e, \quad (34)$$

instead of Eq. (30).

6.3. Quantum Approach to γ_s

The γ_s is a quantity of the same dimension as the (angular) frequency. In reality, its value should be obtained on the basis of a microscopic quantum theory. It is awaited that γ_s depends on the fundamental quantum constant \hbar , the Planck constant. Klačka and Kocifaj ([3] Eq. (26)) used the formula

$$\gamma_s \approx k_B T / \hbar, \quad (35)$$

see also Eq. (27).

6.4. Comparison

Comparison of the results represented by Eq. (30) and Eq. (35) yields for the case of the water droplet at 20°C $\gamma_s(\text{classical})/\gamma_s(\text{quantum}) = 1.52$. Relating Eq. (34) and Eq. (35) for the water droplet at 20°C one obtains $\gamma_s(\text{improved classical})/\gamma_s(\text{quantum}) = 1 + (4/3) \times 10^{-2} \approx 1.01$.

6.5. Discussion on γ_s -Parameter

In any case, we have to consider the above presented coincidence (Sec. 6.4) between the numerical values of $\gamma_s(\text{classical})$, $\gamma_s(\text{improved classical})$ and $\gamma_s(\text{quantum})$ as a pure chance. The quantum mechanical approach given by Eq. (35) should be a relevant approximation to reality.

There exists another argument that classical, non-quantum, approach cannot yield results of the kind of Eq. (35). Note that the case $\omega \rightarrow 0$ yields for conductivity $\sigma = Ne^2\tau/m$, $\tau = l/v$, where l is the mean free path. As for the classical physics, it was assumed by Drude and Lorentz that l is independent of temperature and $v = \sqrt{3k_B T/m}$ (see [4], p. 190). The classical physics is not in agreement with experimental conclusions. The real situation can be described, for metals (conductivity of isolants can be an increasing function of temperature), by the relation $\tau^{-1} = \tau_{impurities}^{-1} + \tau_{e-e}^{-1} + \tau_{e-phonon}^{-1} + \dots$ and $\tau_{impurities}^{-1} \propto T^0$, the electron-electron interaction is described as $\tau_{e-e}^{-1} \propto T^2$, the electron-phonon interaction yields $\tau_{e-phonon}^{-1} \propto T^5$ for low temperatures T , and, $\tau_{e-phonon}^{-1} \propto T^1$ for high temperatures T . Similar situation can be awaited for the total γ_s . Thus, approximately, $\gamma_s \propto T$ for metals, conductors.

7. NUMERICAL RESULTS

The differences between classical and quantum physics approaches are documented by set of targeted numerical experiments. For the sake of brevity we introduce two dimensionless quantities: the relative permeability μ_r and $\gamma_{s,factor}$, defined by the relations

$$\mu_1 \equiv \mu_r \mu_0, \quad (36)$$

$$\gamma_s \equiv \gamma_{s,factor} k_B T / \hbar, \quad (37)$$

see also Eq. (35). The $\gamma_{s,factor}$ may be treated as a dimensionless quantity related to the properties of the spherical particle.

Particle optical properties determined by means of classical and quantum physics are documented graphically. Various surface electric potentials of the spherical particle are assumed. The electrically neutral particle is characterized by the surface potential 0V. As it is evident from Figs. 1–7, the optical response of the particle to the incident electromagnetic field depends essentially on the wavelength of the radiation, temperature of the particle, μ_r , refractive index, and the value of $x = 2\pi R/\lambda$. Classical and quantum approaches yield different results, in general. We remind that classical physics is given by Eq. (24), while quantum physics by Eq. (26) and Eq. (37).

Figures 1 and 2 depict ratios of efficiency factors for extinction for charged and neutral particles $Q_{ext}(c)/Q_{ext}(0) \equiv Q_{ext}(c)/Q_{ext}$. The figures hold for almost identical situations except for the refractive index. Small value of the imaginary part of the complex refractive index leads to quite reduced absorption, thus implying different behavior for classical and quantum approaches. This is apparent from

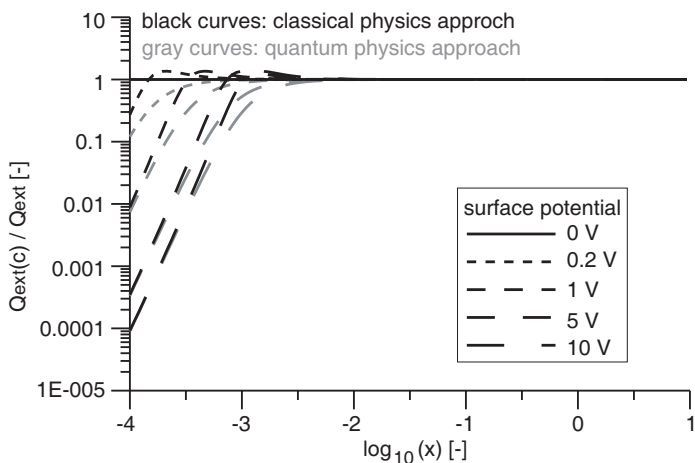


Figure 1. Ratio of extinction efficiency factors for charged and neutral particles as a function of size parameter $x = 2\pi R/\lambda$. The results are obtained for strongly absorbing particles with refractive index $m = 5.0 + 3.0i$ under the following conditions: $\lambda = 5 \mu\text{m}$, $\mu_r = 1.0$, $T = 30 \text{ K}$, $\gamma_{s, factor} = 0.1$.

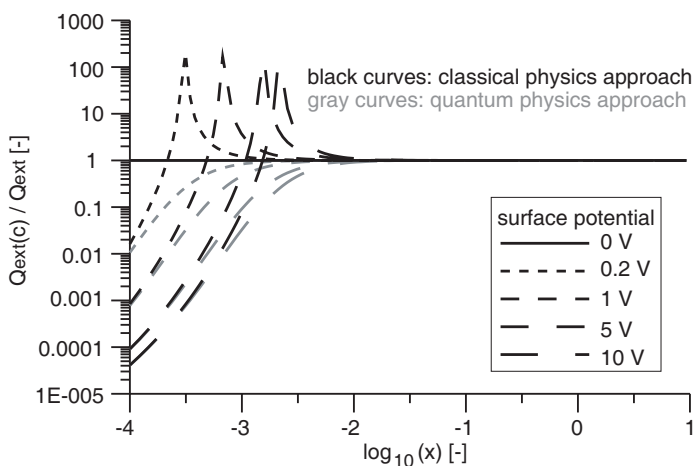


Figure 2. Ratio of efficiency factors for extinction for charged and neutral particles. The slightly absorbing particles with refractive index $m = 2.5 + 0.1i$ are considered. The further computational parameters are as follows: $\lambda = 5 \mu\text{m}$, $\mu_r = 1.0$, $T = 30 \text{ K}$, $\gamma_{s, factor} = 0.1$.

Fig. 1. In the quantum physics approach the ratio of $Q_{ext}(c)/Q_{ext}$ is a smooth and monotonous function of size parameter x , as follows from Figs. 1 and 2. In contrast, the classical approach applied to slightly absorbing particles generates very sharp peaks of $Q_{ext}(c)/Q_{ext}$ with maxima about 100 or more (see Fig. 2).

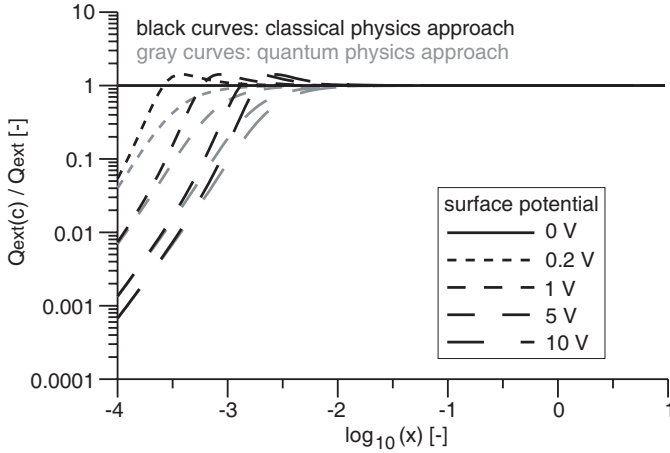


Figure 3. The same as in Fig. 1, but at wavelength $\lambda = 1$ mm and with $\mu_r = 4.0$.

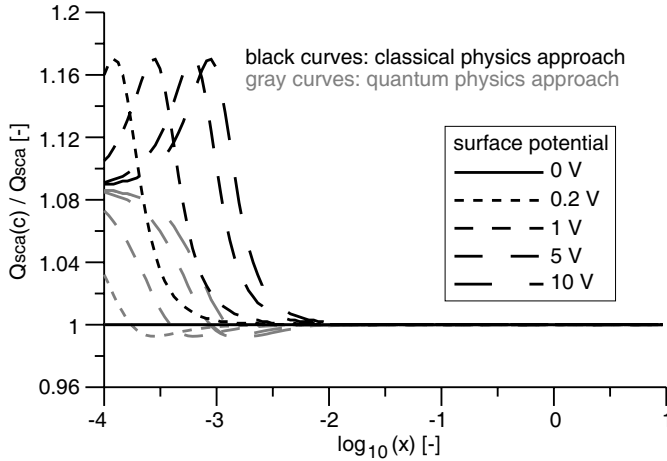


Figure 4. Ratio of efficiency factors for scattering for charged and neutral particles. The results for strongly absorbing particles with refractive index $m = 5.0 + 3.0i$ are obtained under the following setup: $\lambda = 1$ mm, $\mu_r = 1.0$, $T = 30$ K, $\gamma_{s, factor} = 0.1$.

Figure 3 also depicts the ratios of efficiency factors for extinction for charged and neutral particles $Q_{ext}(c)/Q_{ext}$. The Figs. 1 and 3 differ in the value of μ_r . Both of the figures confirm the general trend that the maxima of the presented curves occur for higher values of x when higher values of surface electric charges exist.

Figure 4 presents the ratios of efficiency factors for scattering for charged and neutral particles $Q_{sca}(c)/Q_{sca}(0) \equiv Q_{sca}(c)/Q_{sca}$. While the classical physics approach results in weak resonances, the quantum physics approach suggests a quick balancing of the scattering efficiencies of charged and neutral particles. The backscattering features of $Q_{bk}(c)/Q_{bk}$ are similar to those for scattering.

Figures 5 and 6 depict ratios of efficiency factors for radiation pressure for charged and neutral particles $Q_{pr}(c)/Q_{pr}(0) \equiv Q_{pr}(c)/Q_{pr}$. Absorption (related to the imaginary part of the refractive index) and

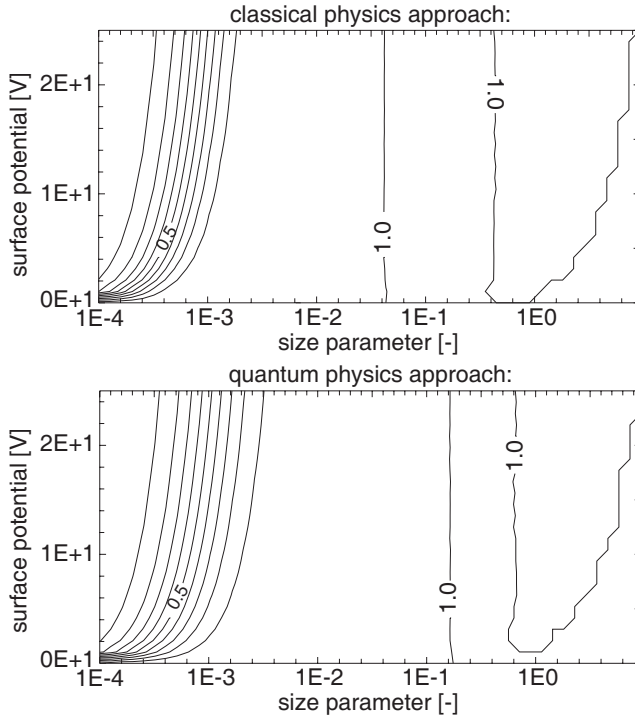


Figure 5. Isolines represent the ratio of efficiency factors for radiation pressure for charged and neutral particles. The strongly absorbing particles with refractive index $m = 5.0 + 3.0i$ at $\lambda = 1$ mm are considered. The rest parameters are $\mu_r = 1.0$, $T = 30$ K, but now $\gamma_{s, factor} = 1.0$.

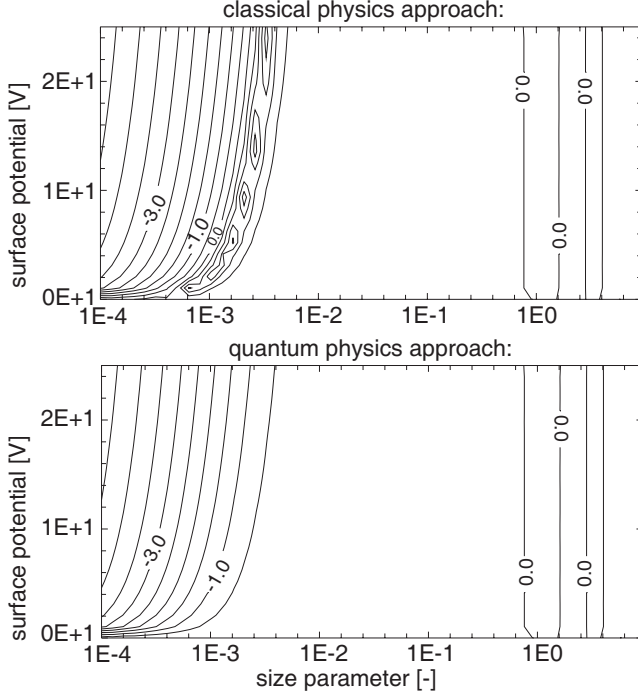


Figure 6. Isolines represent the decadic logarithm of the ratio of efficiency factors for radiation pressures $Q_{pr}(c)/Q_{pr}(0)$. Here $Q_{pr}(c)$ corresponds to the charged particles, while $Q_{pr}(0)$ is obtained from convenient Mie theory for electrically neutral particles. The slightly absorbing particles with refractive index $m = 2.5 + 0.1i$ at $\lambda = 5 \mu\text{m}$ are considered. The rest computational parameters are $\mu_r = 1.0$, $T = 30 \text{ K}$, $\gamma_{s, factor} = 0.1$.

the values of $\gamma_{s, factor}$ of the particles are different. Similarly to the results presented in the previous figures, the slope of $Q_{pr}(c)/Q_{pr}$ determined under classical physics conditions is much steeper than in the case of quantum physics approach (consult Figs. 5 and 6). The resonance peaks exist only for classical approach when the slightly absorbing material is considered (Fig. 5).

Figure 7 depicts Q_{pr}/Q_{ext} as a function of $\log x$ for various combinations of optical parameters. The difference between charged and neutral particles is small. Also the results for quantum and classical physics approaches are almost identical (and thus not separated in Fig. 7). The figure immediately implies $0 \leq Q_{pr}/Q_{ext} \leq 1.2$, which is consistent with relativity theory $0 \leq Q_{pr}/Q_{ext} \leq 2$, although Q_{pr} may be greater than 2 [14].

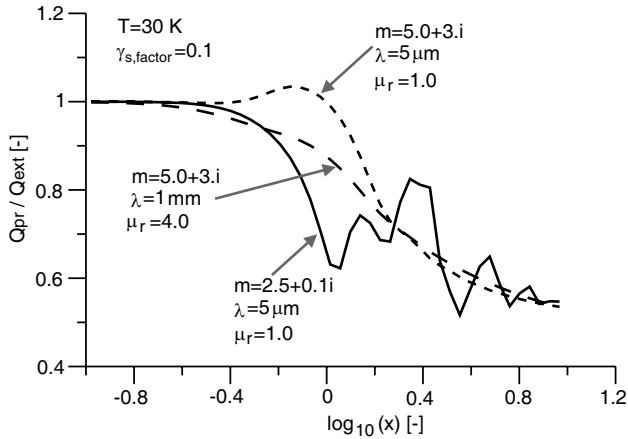


Figure 7. Efficiency factor for radiation pressure to efficiency factor for extinction as a function of the size parameter $x = 2\pi R/\lambda$.

8. CONCLUSION

The Mie’s solution of the Maxwell’s equations is generalized to an interaction of an incident electromagnetic radiation with electrically charged sphere. The paper presents relevant equations for calculating optical properties of the charged spherical particles (Eqs. (6)–(9)). The classical physics (Eq. (24)) as well as the quantum physics (Eqs. (26) and (37)) approaches are treated and documented in set of numerical simulations. The targeted computations were made for charged spherical particles with various values of permeability, refractive index, wavelength of the incident radiation, surface charge, temperature, and other physical parameters. It is shown that classical and quantum physics approaches may provide different results, especially when the particles are composed of slightly absorbing materials. An inconsistency of both approaches is most important for scattering and backscattering features. While the classical approach may generate very sharp resonance peaks, the size-dependent optical properties (like efficiency factors for scattering, extinction and radiation pressure) show quite smooth and rather monotonous behavior in the case of quantum physics approach. Increasing the wavelength, the surface resonances continuously disappear. As the particle size becomes several orders of magnitude smaller than the wavelength of the incident radiation, the charged particle tends to remove much less electromagnetic energy than that of Mie’s (neutral) particle, i.e., $Q_{ext}(charged)/Q_{ext}(neutral) \ll 1$. This is generally related to a reduced absorption efficiency. As shown in Fig. 7, the presence of absorbing materials in a particle may

result either in removal of ripple resonance structure, or in a shift of the resonance maxima (or both of these things are the case).

Our results show that classical and quantum physics approaches are consistent in the long wave region, but relevant differences exist in the intermediate spectral region. The found discrepancy between classical and quantum approaches is a sufficient motivation for experimentalists to verify if what is theoretically derived is the same as what is measured in laboratory. Materials with enhanced conductivities can be used in experiments to identify the approach, classical or quantum, which provides results consistent with measurements.

Heifetz et al. [5] have performed set of experiments on millimeter-wave scattering from neutral and charged water droplets. The measurements confirmed an increased scattering efficiency for droplets smaller than 100 nm, which is consistent with our theoretical findings. Heifetz and his team also outlined some potential applications in remote sensing of radioactive gases that are emitted as byproducts of nuclear fuel cycle reactions.

ACKNOWLEDGMENT

J.K. was partially supported by the Scientific Grant Agency VEGA, grant No. 2/0016/09.

REFERENCES

1. Mie, G., "Beiträge zur optik trüber medien speziell kolloidaler metalösungen," *Ann. Phys.*, Vol. 25, 377–445, 1908.
2. Bohren, C. F. and A. J. Hunt, "Scattering of electromagnetic waves by a charged sphere," *Can. J. Phys.*, Vol. 55, 1930–1935, 1977.
3. Klačka, J. and M. Kocifaj, "Scattering of electromagnetic waves by charged spheres and some physical consequences," *J. Quant. Spectroscopy & Radiative Transfer*, Vol. 106, 170–183, 2007
4. Pillai, S. O., *Solid State Physics*, 6th edition, New Age Science, Tunbridge Wells, Kent, UK, 2010.
5. Heifetz, A., H. T. Chien, S. Liao, N. Gopalsami, and A. C. Raptis, "Millimeter wave scattering from neutral and charged water droplets," *J. Quant. Spectroscopy & Radiative Transfer*, 2010, doi:10.1016/j.jqsrt.2010.08.001.
6. Mishchenko, M., L. D. Travis, and A. A. Lacis, *Scattering*,

- Absorption and Emission of Light by Small Particles*, Cambridge University Press, Cambridge, UK, 2002.
7. Mishchenko, M. I., "Far-field approximation in electromagnetic scattering," *J. Quant. Spectroscopy & Radiative Transfer*, Vol. 100, 268–276, 2006.
 8. Harada, Y. and T. Asakura, "Radiation forces on a dielectric sphere in the Rayleigh scattering regime," *Optics Comm.*, Vol. 124, 529–541, 1996.
 9. Rosenkrantz, E. and S. Arnon, "Enhanced absorption of light by charged nanoparticles," *Opt. Lett.*, Vol. 35, 1178–1180, 2010.
 10. Dressel, M. and G. Grüner, *Electrodynamics of Solids: Optical Properties of Electrons in Matter*, Cambridge University Press, Cambridge, UK, 2002.
 11. Meschede, D., *Optics, Light and Lasers*, 2nd edition, 88, Wiley-VCH Verlag, Weinheim, 2007.
 12. Giaquinta, M. and G. Modica, *Mathematical Analysis: An Introduction to Functions of Several Variables*, 227–228, Birkhäuser, a Part of Springer Science+Business Media, LLC, Boston, 2009.
 13. Lyle, S. N., *Self-Force and Inertia: Old Light on New Ideas*, Springer-Verlag, Berlin, 2010.
 14. Klačka, J., "Electromagnetic radiation, motion of a particle and energy-mass relation," arXiv: astro-ph/0807.2915, 2008.
 15. Sabah, C. and S. Uckun, "Multilayer system of Lorentz/Drude type metamaterials with dielectric slab and its application to electromagnetic filters," *Progress In Electromagnetic Research*, Vol. 91, 349–364, 2009.
 16. Koledintseva, M.-Y., R.-E. DuBroff, R.-W. Schwarts, and J.-L. Drewniak, "Double statistical distribution of conductivity and aspect ratio of inclusions in dielectric mixtures at microwave frequencies," *Progress In Electromagnetic Research*, Vol. 77, 193–214, 2007.
 17. He, S., Z. Nie, and J. Hu, "Numerical solution of scattering from thin dielectric-coated conductors based on TDS approximation and EM boundary conditions," *Progress In Electromagnetic Research*, Vol. 93, 339–354, 2009.
 18. Sha, W.-E.-I. and W.-C. Chew, "High frequency scattering by an impenetrable sphere," *Progress In Electromagnetic Research*, Vol. 97, 291–325, 2009.
 19. Censor, D., "Relativistic electrodynamics: Various postulate and ratiocination frameworks," *Progress In Electromagnetic Research*, Vol. 52, 301–320, 2005.